

THE FUNDAMENTAL POWER COUPLER FOR CEPC BOOSTER CAVITY*

T. Huang[†], F. Bing, R. Guo, H. Lin, Q. Ma, W. Pan, J. Zhai, Z. Zhang
 Institute of High Energy Physics (IHEP), Beijing, China

Abstract

96 Tesla type 1.3GHz 9-cell superconducting cavities, housed in eight 12m-long cryomodules, will be adopted for CEPC booster. Each cavity equips with one variable, double-window fundamental power coupler (FPC). The FPC will operate at RF power up to 20 kW at quasi-CW mode. A variable coupling from 4E6 to 1E7 is required to meet different operation modes of Higgs, W and Z. A new coupler that employs a 50 Ohm coaxial line with bellow structures, a cylindrical warm window, a coaxial planar cold window and a coupling adjusting actuator has been designed. Then two prototypes have been fabricated and high power tested up to CW 70 kW. In this paper, the design, fabrication and high power test of the prototype FPCs will be presented.

INTRODUCTION

The Circular Electron Positron Collider (CEPC) is an electron positron collider operating at 90-240 GeV center-of-mass energy of Z, W and Higgs bosons, located in a 100-km circumference underground tunnel [1]. The accelerator complex consists of a linear accelerator, a damping ring, the booster, the collider and several transport lines. The booster provides electron and positron beams to the collider at different energies required by the three collider operating modes (Z, W and Higgs).

The SRF system parameters of the CEPC Booster Ring is described in reference [1]. 96 Tesla type 1.3GHz 9-cell superconducting cavities, housed in eight 12m-long cryomodules, will be adopted for CEPC booster. Each cavity equips with one fundamental power coupler (FPC). A maximum RF power of 20 kW (Peak) and 4 kW (Average) is required to be delivered by the FPC. The different requirements at Z, W and H operation have imposed the use of a variable coupling power coupler with a Q_e value varying from 4E6 to 1E7. The main requirements of the booster FPC are summarized in Table 1.

Initially, the coupler was developed for a pure R&D project aiming for variable, clean assembly and high average RF power up to 75kW. Since the power, Q_e range and interfaces fulfilling the requirements of the CEPC booster cavity, it was adopted as the CEPC booster FPC later. The coupler features as a cylindrical warm window and a Tristan-type cold window. Two prototypes have been fabricated and high power tested up to CW 70 kW. In this paper, the design, fabrication and high power test of the prototype FPCs will be presented.

* Work supported by National natural Science Foundation of China (11475203)

[†] huangtm@ihep.ac.cn

Table 1: The Main Requirements of the Booster FPC

Parameters	Value
Frequency	1.300 GHz
Power	20 kW(Peak); 4 kW (Average)
Q_e	4E6 to 1E7
2 K heat loss	0.06W (Dynamic, 4kW, CW, TW)
Assembly	Coupler and cavity assembled in class 10 clean room

DESIGN

In order to be assembled with the cavity in class 10 clean room, the FPC is designed with two windows: one warm window and one cold window. The warm window is derived from TTF-III coupler [2] and the cold window is belonging to the Tristan-type family [3]. The 3D half model of the CEPC booster coupler is shown in Fig. 1. The coupler consists of several sub-assemblies shown in Fig. 2. The main assemblies are the cold part, the warm outer and inner coaxial sub-assemblies, the demountable warm window, the waveguide-coaxial transition and the tuning mechanism.

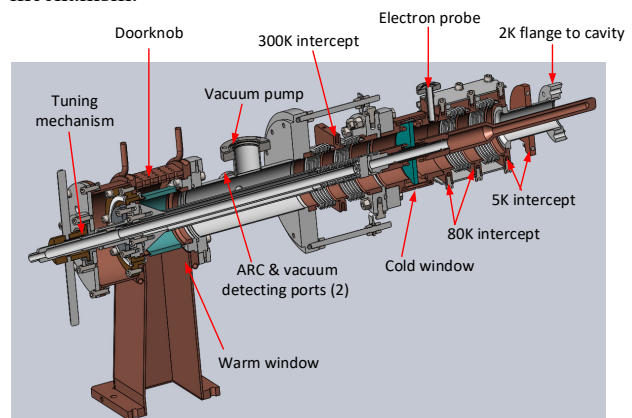


Figure 1: The FPC for CEPC booster cavity.

Compared with TTF-III coupler, a series of modifications have been made to handle a higher average power and achieve a more safe operation:

1. The warm window size is enlarged, with outer diameter of 87mm.
2. The cold part is completely redesigned by applying a Tristan-type window.
3. Forced air cooling is added to the inner conductor of the warm coaxial line.
4. Both air and water cooling are applied to the warm window.
5. The warm window is designed to be demountable for easy replacement once damaged.

Content from this work may be used under the terms of the CC BY 3.0 licence (© 2019). Any distribution of this work must maintain attribution to the author(s), title of the work, publisher, and DOI.

- A DC bias voltage mechanism is arranged to suppress potential Multipacting effect.

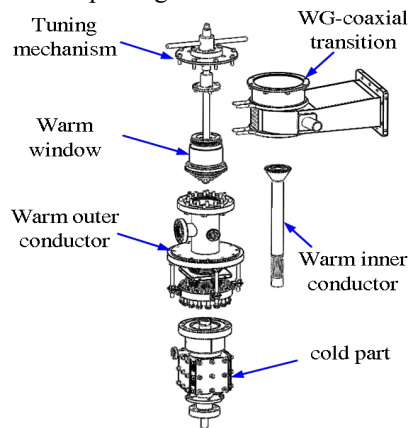


Figure 2: Exploded view of the coupler.

In addition, the antenna excursion is designed to be 20 mm to meet the coupling adjusting requirement.

Figure 3 shows the simulated power transmission performance of the whole coupler assembly. The S11 is better than -54 dB at the operation frequency. The electric and magnetic field distribution when 75 kW CW RF power passes through in TW mode is shown in Fig. 4. The maximum electric field is 7E5 V/m, one fourth of the air breakdown value.

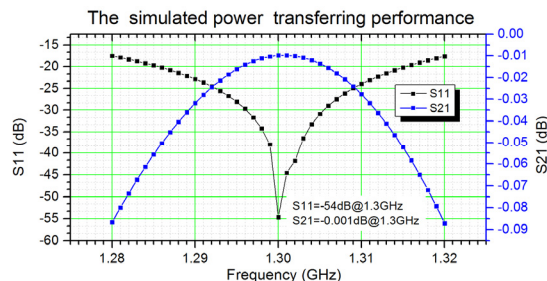


Figure 3: The simulated power transferring performance of the whole coupler assembly.

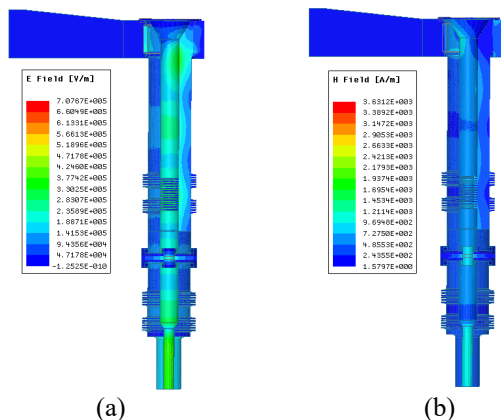


Figure 4: The electric (a) and magnetic (b) field when 75 kW CW RF power passes through in TW mode.

Simulations of Multipacting in the FPC were carried out using CST [4]. The coupler was divided into four parts for the Multipacting simulation, which indicated as the particle

sources location showing in Fig. 5. The magnitude of the input power was swept from 0 to 80 kW with step of 5 kW, and the phase swept from 0 to 330 degree with step of 30 degree. The Multipacting was estimated by the ratio of the secondary enhancement current and the initial current '<SEY>'. Multipacting is possible when '<SEY>' exceeds one. The simulation results show that there is no hard barrier under 80 kW, as shown in Fig. 6.

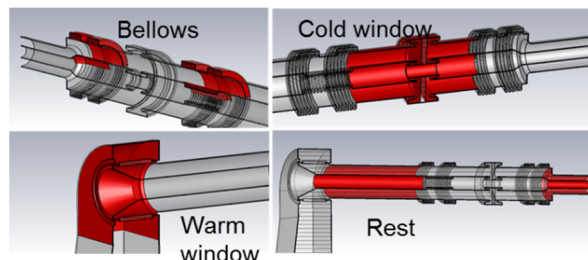


Figure 5: The particle sources location used in the Multipacting simulation.

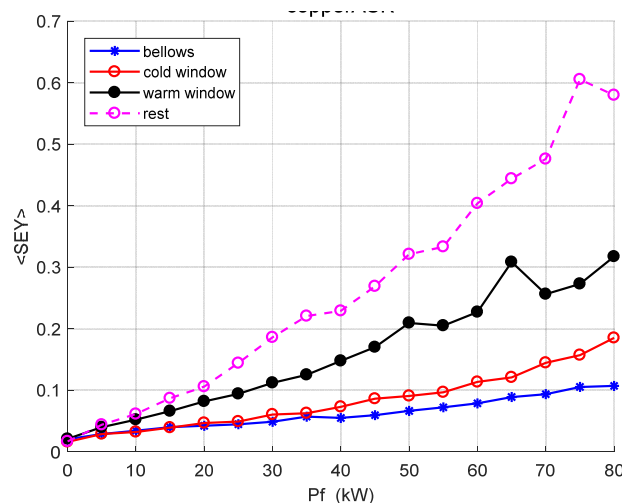


Figure 6: The Multipacting simulation results of each part of the coupler.

Dedicated RF-thermal analysis were done by ANSYS Workbench [5], focusing on the bellow temperature and the cryogenic heat loss. By adding one 298K thermal intercept at the warm outer bellow, two 80K thermal intercepts at the cold outer bellow and forced air cooling of the warm inner conductor, the temperature of the bellows decreased significantly. In addition, both forced air and water cooling are applied to the warm window. Figure 7 shows the calculated temperature distribution at the power of CW 75 kW in traveling wave (TW) mode. Except for the inner conductor of the cold part made of solid copper, all the coaxial line parts were made of stainless steel with copper plating on the RF surfaces. The thickness and the RRR value of the copper plating were optimized to minimum the cryogenic heat loss. Figure 8 shows the 2K heat loss contributed by the FPC at different RRR values of the copper plating. It can be seen that the static 2K heat loss decreases as the RRR value decreasing; however, the dynamic heat loss increases as the RRR decreasing. Thus

there is an optimum RRR value corresponding a specified RF power level. Based on the simulation, the optimum RRR value is 30 and 50 for CW 4kW and 75kW respectively. Table 2 lists the calculated static and dynamic heat loss and the temperature of key components at CW 4kW and 75kW in TW mode.

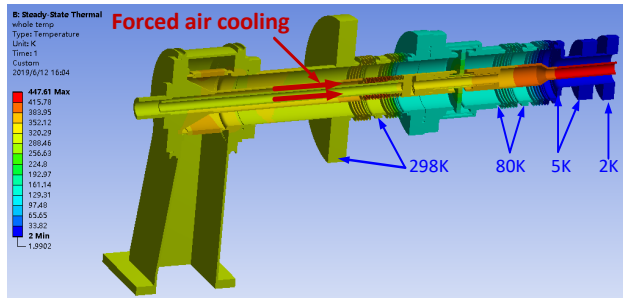


Figure 7: The calculated temperature distribution at the power of CW 75 kW in TW mode.

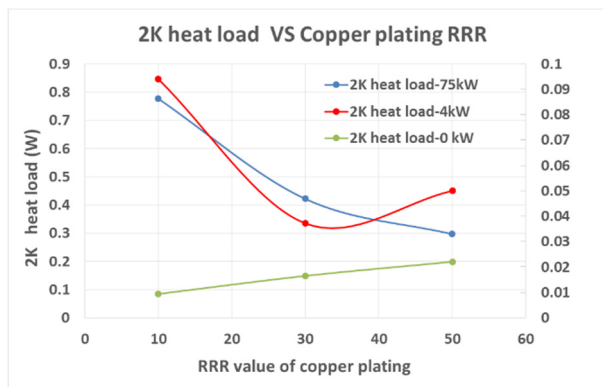


Figure 8: The 2K heat loss contributed by the FPC at different RRR value of the copper plating.

Table 2: The calculated static and dynamic heat loss and the maximum temperature of key components at CW 4kW and 75 kW in TW mode.

Items	Static		Dynamic	
	RRR=30 0 kW	RRR=30 4 kW	RRR=30 4 kW	RRR=30 75 kW
2 K heat loss (W)	0.02	0.037	0.037	0.42
5 K heat loss (W)	3.40	3.51	3.51	5.71
80 K heat loss (W)	16.2	21.7	21.7	142
Warm OC bellow T (°C)	25	27	27	66
Warm IC bellow T (°C)	23	24	24	125
Cold bellow T (°C)	-143	-142	-142	-109
Warm window T (°C)	23	26	26	90
Cold window T (°C)	-114	-108	-108	37

FABRICATION

Two prototype couplers have been manufactured at HERT (High Energy Racing Technology). HERT was responsible for most of the manufacturing processes except for the copper plating which completed at AHPTI (Anhui Huadong Polytechnic Institute).

Window brazing and copper plating has been proved to be two critical and challenging manufacturing processes. The windows were brazed in a vacuum furnace at 800°C with Ag72Cu28. Both the sequences and the temperature evolutions play an important role in the success of window brazing. The cold window brazing processes were reduced from 3 steps to 2 steps shown in Fig. 9, which increased the success rate greatly. Figure 10 gives the optimized temperature evolution curve of the window brazing.

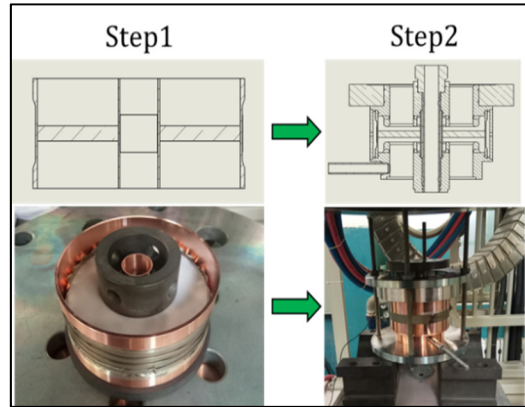


Figure 9: The cold window brazing processes.

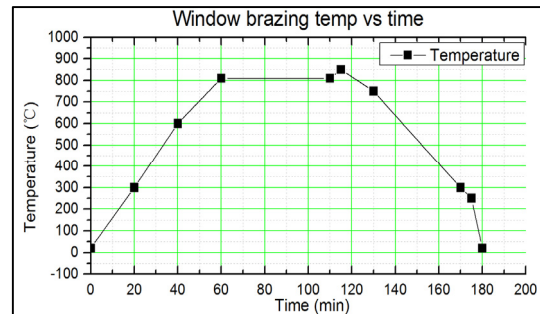


Figure 10: The temperature evolutions of the window brazing.

The copper plating was processed after parts brazing or welding. The requirements for thickness, RRR value, good uniform, adhesiveness and cleanliness make the copper plating particularly challenging. The electrode has been improved constantly to obtain a qualified thickness uniformity, especially for the bellow structures. Finally, we got a good uniformity within 20% as shown in Fig. 11. The adhesiveness was tested by liquid nitrogen shocking and ultrasonic cleaning. Figure 12 shows the fabricated sub-assemblies and the whole assemblies of the coupler.



Figure 11: The measured copper plating thickness of the warm OC bellow: (a) peak: 29um; (b) valley: 26um.

Content from this work may be used under the terms of the CC BY 3.0 licence (© 2019). Any distribution of this work must maintain attribution to the author(s), title of the work, publisher, and DOI.

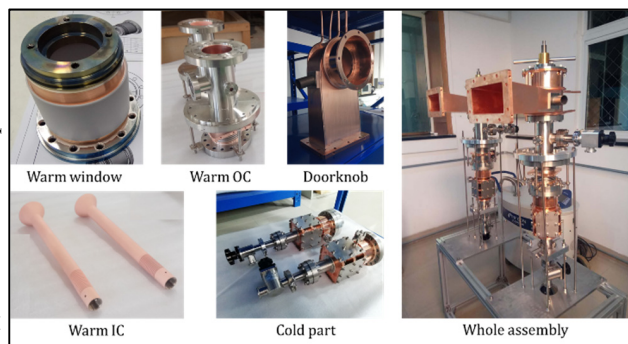


Figure 12: The fabricated sub-assemblies and whole assemblies of the coupler.

HIGH POWER TEST

Usually, the FPC should be high power tested on the test bench before assembled with the cavity. This operation is very important for two reasons. One is to remove the residual gases, dust and invisible particles by RF power, which helps avoid the contamination of the SRF cavity; the other is to verify the coupler performances during high power operation, including thermal, vacuum and RF activities [6].

Preparation and Assembly

A high power source was not available at the time of the prototype couplers test. Therefore, the high power test has been processed at a resonant ring platform developed at Peking University [7]. The coupler high power test setup is shown in Fig. 13. A 1.3GHz, CW 10 kW SSPA was used. The coupler test stand, with two couplers connected by a waveguide box, was inserted in the resonant ring, which had a RF power gain of about 5 to 8 times.

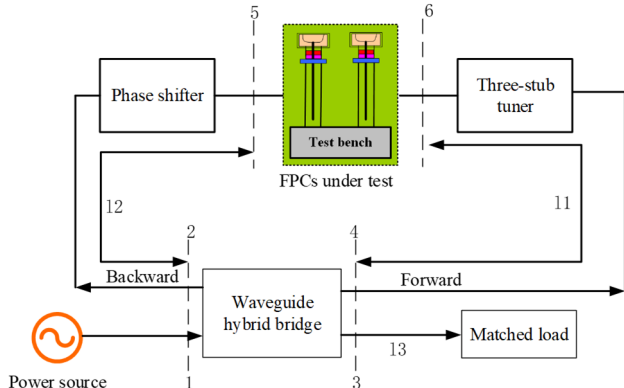


Figure 13: The coupler high power test setup.

Prior to the test, the couplers were cleaned according to a dedicated cleaning procedure: 1) Ultra-sonic cleaned with detergent at 50 °C; 2) Rinsed with ultra-pure water; 3) Dried by dust-free nitrogen gas. Then, the vacuum components were assembled in a Class 10 clean room (Fig. 14a), and baked at 120 °C for 48 hours. After that, the test stand were transported to Peking University under vacuum, then installed with the cooling setup and the instrument elements such as vacuum gauges, arc detectors, electron probes and temperature sensors (Fig. 14b). Figure 15

shows the cooling setup used in the high power test. The cold outer conductor was cooled by the thermal intercepts connected to liquid Nitrogen pipes cooled copper plates.

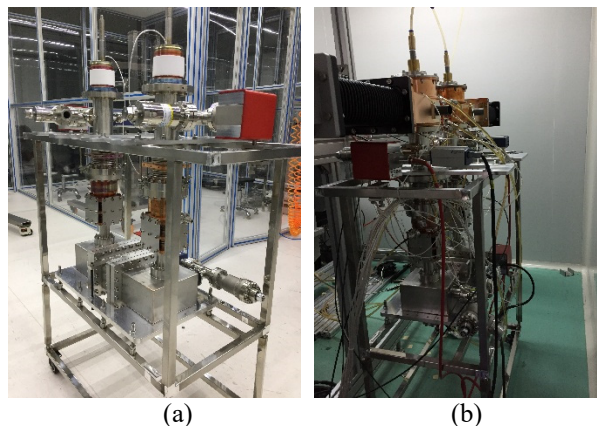


Figure 14: The assembly of the coupler test stand: (a) clean assembly; (b) on-site installation.

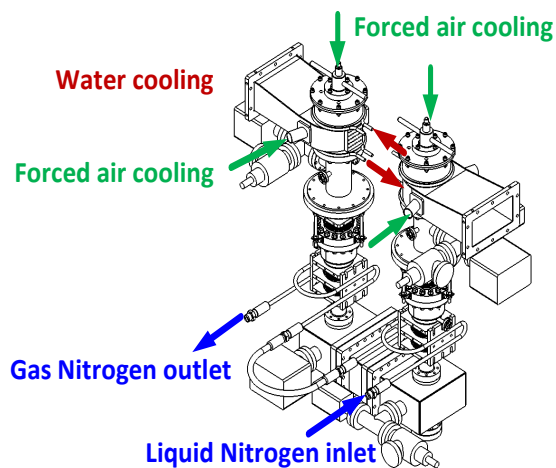


Figure 15: The cooling scheme during the high power test.

The antenna excursion “L_{antenna}” for Q_e adjusting was tested to be ±10 mm, as shown in Fig. 16, corresponding to a variable Q_e from 1.5E6 to 1E8, which well covered the CEPC booster cavity requirement.

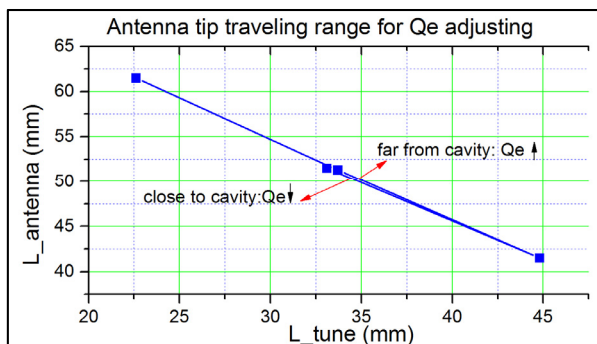


Figure 16: The antenna tip traveling range for Q_e adjusting was tested to be ±10 mm.

High Power Conditioning

The high-power conditioning started with low duty factor (DF) at 10Hz. Then the DF was increased by gradually extending the pulse width and eventually reached CW. RF interlock was added to protect the coupler against bad vacuum, arc discharging and over-heating. An automatic conditioning program was developed, with the function of RF power controlling according to the vacuum, fast interlocks, remote operation and data archiving. Figure 17 shows the RF conditioning method. Three vacuum thresholds were set in the program; and the RF power was automatically increased or decreased according to the following algorithm. If the vacuum was between the low level (5E-5 Pa) and the middle level (1E-4Pa), the power amplitude was kept constant. If the vacuum was between the middle level and the high level (5E-4 Pa), the RF power was reduced at a setting rate. If the vacuum was worse than the high level, the RF power was switched off. When the vacuum was better than low level, the RF power was switched on and increased at a setting rate.

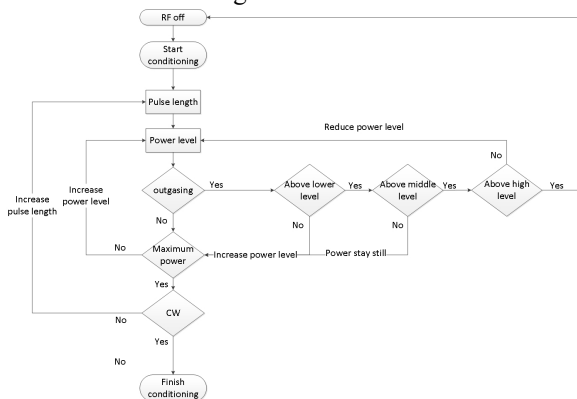


Figure 17: The RF conditioning method.

The initial conditioning with pulse width of 10 us took the longest time, as can be seen from the statistics of the time elapsed at each pulse width shown in Fig. 18. Figure 19 shows the vacuum evolution during the whole conditioning. The vacuum between two cold windows and the connecting waveguide box was worse than the vacuum of both warm sides. That's because the baking temperature of the connecting box was only 80°C due to poor copper plating of the box. After 60 hours conditioning, two prototypes reached CW 70kW. No arc discharging was observed during the whole conditioning process. Also no hard Multipacting barrier was found after conditioning, which agreed well with the simulation.

One of the main purpose is to check the temperature rise of the coupler at high average power levels. More than 10 temperature sensors of Pt100 were arranged at the critical parts of the coupler, as shown in Fig. 20. Though the maximum RF power reached was CW 70kW, it was difficult to keep the resonant ring tuned for more than 30 minutes as the power above CW 50kW due to the thermal drift. So we lowered the RF power and stayed at 30kW for 60 minutes and 40kW for 30 minutes. Table 3 lists the

equilibrium temperatures when staying at 40kW for 30 minutes. A maximum temperature up to 103°C at the inner conductor of the warm part was observed, which far above the simulation result of 72 °C . We speculate the overheating was caused by poor copper plating and insufficient cooling of the warm inner conductor. Further improvements will be implemented by modifying the cooling design and improve the copper plating.

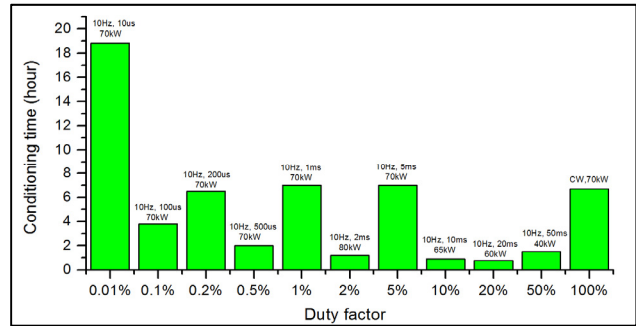


Figure 18: The statistics of the time elapsed at each pulse width.

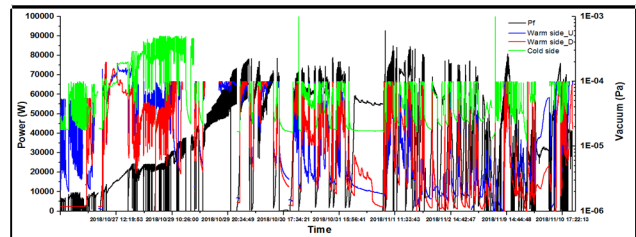


Figure 19: The whole conditioning history: forward RF power (black); upside warm vacuum (blue); downside warm vacuum (red); cold side vacuum (green).

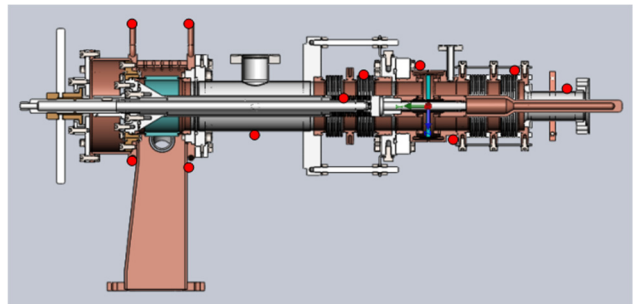


Figure 20: The temperature sensors Pt100 distribution.

Table 3: The Equilibrium Temperatures When Staying at 40kW for 30 Minutes

Location	Temperature up./down. (°C)
Inlet water	21.1/22.5
Outlet water	21.7/23.7
Doorknob WG up	25.2/27.2
Doorknob WG down	24.7/25.3
Warm inner conductor	97.2/102.7
Warm outer conductor	19.1/30.0
Warm outer bellow	58/74.2
Cold window up	18.9/-24.6
Cold window down	15.6/-35.4
Cold outer bellow	14.4/-35.5
Connecting box	52.5/50.7

SUMMARY

A 1.3GHz variable, double-window coupler aiming for transferring a CW RF up to 75 kW has been developed at IHEP, which can be applied in CEPC Booster cavity. Two prototypes have been fabricated and high power tested on the test benches. A maximum of CW 70kW RF power has been reached. Due to thermal drifting of the resonant ring, the RF power was lowered below 50kW for power keeping test. After staying at 40 kW for 30 minutes, a temperature up to 103°C at the inner conductor of the warm part was observed, which far above the simulation result of 72 °C. The possible reasons are poor copper plating and insufficient cooling of the warm inner conductor. Further improvements will be implemented by modifying the cooling design and improve the copper plating.

REFERENCES

- [1] The CEPC Study Group, “CEPC Conceptual Design Report”, Volume 1-Accelerator, August 2018.
- [2] B. Dwersteg, D. Kostin *et al.*, TESLA RF Power Couplers Development at DESY, in *Proceedings of the 10th Workshop on RF Superconductivity*, Tsukuba, Japan, 2001.
- [3] T. Furuya, Y. Kijima, S. Mitsunobu, T. Tajima, and T. Tanaka, “Input Coupler of the Superconducting Cavity for KEKB”, in *Proc. 7th European Particle Accelerator Conf. (EPAC'00)*, Vienna, Austria, Jun. 2000, paper THP1A11.
- [4] CST, <https://www.cst.com/>
- [5] ANSYS, <http://www.ansys.com/>
- [6] Tongming Huang, Weimin Pan *et al.*, “High power input coupler development for BEPCII 500MHz superconducting cavity”, *Nuclear Instruments and Methods in Physics Research A*, vol. 623, pp. 895-902, 2010.
- [7] Dehao Zhuang, Yunqi Liu, Fang Wang *et al.*, “An alternative way to increase the power gain of resonant rings”, *Review of scientific instruments* 89, 034702 (2018).